Inertial Labs
a VIAVI Solutions company



Performance Analysis Report

Radio-Aided Inertial Navigation System

October 2025

Table of Contents

1. Abstract 3
2. Scope and Applicability 4
3. Introduction 5
4. Framework for Tests 8
5. Standard Flight Test Outcomes 11
6. Flight Test Results Using Two Radios 16
7. Conclusion 20
8. Bibliography 21
8. Revision History 22

1. Abstract

The RINS (Radio-Aided Inertial Navigation System) Performance Analysis Report evaluates the effectiveness of integrating RF ranging with inertial navigation for positioning in GNSS-denied environments. The system, developed by Inertial Labs, a Viavi Soutions Company (IL) in collaboration with Domo Tactical Communications (DTC), combines a tightly coupled INS with SDR-based RF ranging to provide reliable positioning where GNSS is unavailable or disrupted.

Flight tests were conducted using a Cessna 172S to assess the accuracy and reliability of the system. Results demonstrated that the RF-based positioning method maintains an RMS position error of 92 meters in GNSS-denied conditions. Further tests with a reduced number of radio nodes (two instead of three) showed promising accuracy with a mean error of approximately 200 meters. The system effectively mitigates navigation drift and ensures robust performance by leveraging Kalman filtering and sensor fusion techniques.

The report concludes that RINS provides a viable alternative navigation solution for unmanned aerial vehicles and other applications operating in contested GNSS environments.

Table 1.1.

	Test 1	**Test 2**
GNSS Denied RMS error	92 m	200 m
Radio measurement precision	<40 m	<60 m
Radio nodes	3	2

2. Scope and Applicability

For years the traditional positioning, navigation, and timing (PNT) industry has been heavily reliant on multi-constellation Global Navigation Satellite Systems (GNSS) for aerial applications. In an era of electronic warfare, this dependence becomes precarious as GNSS jamming and spoofing pose a threat to these systems in real-world use cases. This prompts the need for resilient alternative navigation (ALTNAV) solutions for defense purposes. These systems must continuously provide accurate navigation information and time synchronization outputs irrespective of GNSS availability. IL and DTC have leveraged their respective expertise to produce such a solution. This tightly integrated RF ranging, and inertial solution allows for reliable UAV navigation in GNSS denied environments.

3. Introduction

3.1. Sources of GNSS Interference

GNSS is a preferred aiding data source for navigation systems due to its ability to provide dependable data for a fused orientation, position, velocity, and timing (OPVT) solution. However, its susceptibility to disruptions is a major drawback for these systems. In land-based applications, these take the form of tunnels, bridges, and urban environments – instances in which GNSS antennas do not have a clear view of the sky. This does not apply to aerial use cases, as these are instead a victim of artificial interference efforts in most instances.

One key interference source in aerial applications is GNSS jamming. This involves the dissemination of a simple interference signal at a level that makes it incredibly difficult to process GNSS signals. In these situations, the jammer transmits a much stronger signal than the true GNSS signal along a similar frequency band. This results in the INS being unable to properly interpret the satellite signal [1].

Similarly, spoofing attacks generate counterfeit GNSS signals to manipulate the target receiver's reported position, velocity, and time. These attacks can be successful against a variety of GNSS receivers despite using only low-cost equipment. Spoofing remains a modern threat to navigation systems despite efforts to make GNSS waveform modulations more unpredictable [2].

3.2. Description of the System

IL has strategically partnered with DTC™ to combine their expertise in the development of software defined radios (SDRs). These radios perform RF ranging by generating low probability of interception/detection (LPI/LPD) mesh-based time of flight (ToF) packets. These serve as aiding data streams for IL's cutting-edge inertial navigation solutions capable of performing advanced sensor fusion for GNSS-denied position triangulation. The result of this synergized effort is the radio-aided inertial navigation system (RINS). This robust, fused solution simultaneously blends aiding data inputs from multiple PNT sources, and provides users with a single, highly accurate, GNSS-independent navigation solution.

3.2.1. Component Overview

As a standalone solution, the Inertial Labs™ INS is a high-performance strapdown system that determines position, velocity, and absolute orientation with the following parts:

- IL MEMS-based IMU
- Advanced GNSS receiver
- Navigation computer with fusion algorithm based on a robust Kalman Filter (KF) to fuse multiple data sources into a unified solution

This is a dependable means of collecting OPVT information in GNSS-enabled environments. However, when GNSS interference is present the system must rely solely on inertial data. This is a viable method only for short periods of time in UAV applications. As this time increases, the position drifts proportionally, resulting in a navigation solution with an unbounded error. As such, a free inertial or dead reckoning solution is not always the best choice for long term GNSS-denied UAV navigation. In these cases, the system needs another source of aiding data to provide an accurate solution.

The DTC BluSDR-30 mesh network consists of multiple radios that serve as base points capable of operating within a range of more than thirty kilometers from another radio mounted on the aircraft. Once powered, the radios automatically send ToF packets to each other using DTC's cutting-edge Mobile Adhoc Network (MANET) to deliver ultra-low latency and end-to-end encrypted ToF estimation. As a result, the onboard SDR obtains real-time ToF data from the base radios as well as their known, instantaneous 3D position coordinates. The sensor fusion algorithm from the INS then utilizes geolocation techniques to triangulate a position estimate. This is based on the raw RF ranges and radio base station coordinates provided in real-time to the mission computer. The solution is LPI/LPD, making it a viable reference source of instantaneous positioning and timing in GNSS-denied or contested environments.

3.2.2. Architecture and Operability

The combination of real-time ToF data, instantaneous positioning reference, and inertial sensing with sensor fusion capabilities creates a solution with limited ambiguity in challenging environments. The aircraft radio obtains each ToF packet within the mesh network. The INS then processes this data with a robust Kalman Filter, which triangulates the vehicle's position from the RF ranges received by two or more ground radios. The unique integration between the INS and DTC's SDRs is superior to other industry solutions without fusion filter capabilities to simultaneously blend aiding data inputs from various alt-PNT sources. This allows the system to provide versatile and reliable navigation solutions tailored to the specific needs of any use case. Refer to Figure 3.1 below for a comprehensive system architecture diagram.

A tightly integrated INS aided by RF-ranging provides key improvements in comparison to their standalone counterparts due to a variety of reasons. The INS navigation computer can output a wider range of UAV navigation parameters due to its ability to receive data from a multitude of sources. These parameters depend on the system configuration

and include orientation, ground/air speed, acceleration, and more. Additionally, the Kalman filter constantly corrects parameter readings from one aiding data source using data from another source. For example, the INS uses the ToF estimates from the BluSDR-30s to correct its ground speed estimates for the aircraft. This method greatly increases the situational accuracy of the solution.

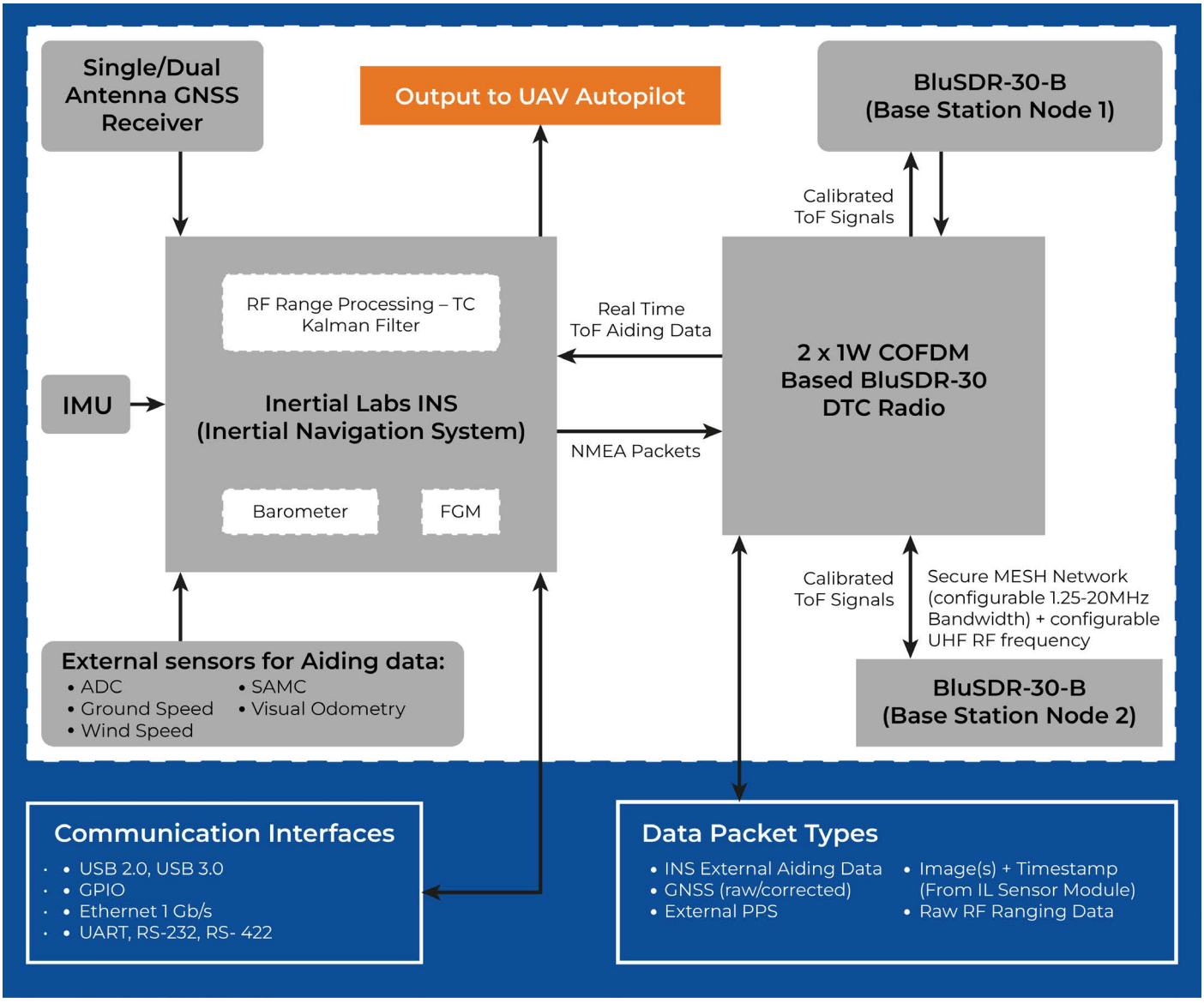


Figure 3.1. RINS System Architecture

4. Framework for Tests

The flight test vehicle used to test this system is a CESSNA 172S. Refer to Figure 4.1 to view the connection scheme for all the RINS components mounted in or on the test vehicle.

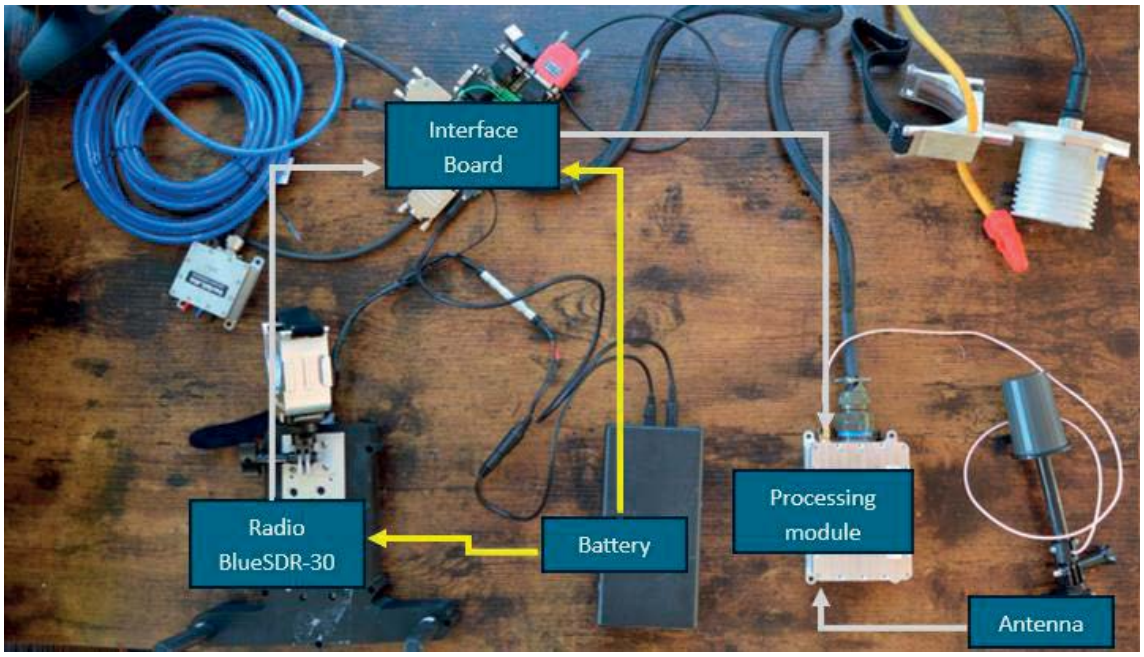


Figure 4.1. Connection Diagram

The complete RINS setup in this test consists of the following items:

- DTC BluSDR-30 Flight Radio
- Battery
- Processing Module and Antenna
- Interface Board

4.1. Radio Setup

Figure 4.2 shows the setup for two of the three BluSDR-30-B base radios on the ground. Ground base 4 (left) and 3 (right) generate an active MESH data link with the UAV radio node. Note the radios are mounted on a tripod and on top of the test vehicle's roof with a clear view of the sky. These precautions increase the quality of the signal and thus provide a better MESH connection.



Figure 4.2. BluSDR-30-B base radios

Figure 4.3 below shows the mounting location for the flight radio. For this test, the radio is on the aircraft's wing strut.



Figure 4.3. Radio Mounted on CESSNA

4.2. Flight Path

Figure 4.4 displays a flight test map with the corresponding latitude and longitude coordinates. Note the three BluSDR-30-B ground node locations placed along the dedicated flight path.

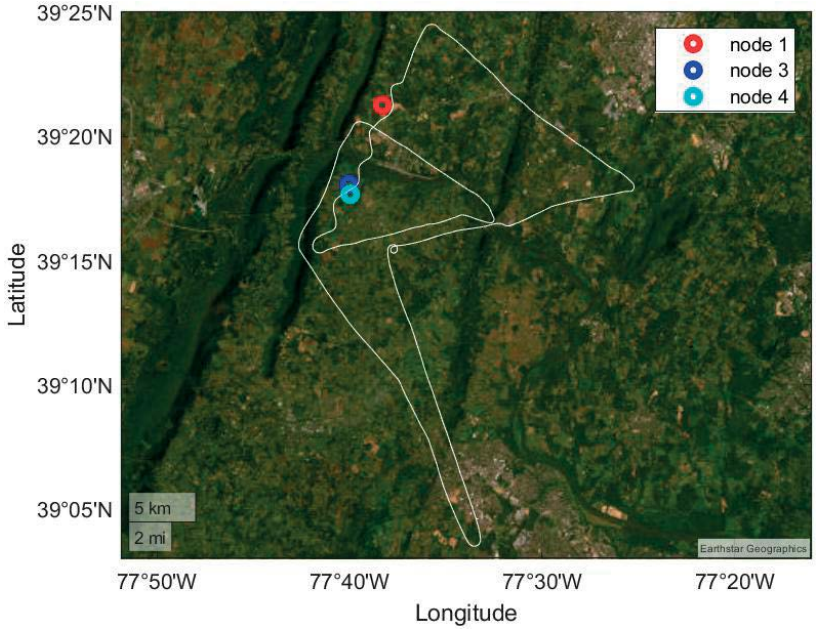


Figure 4.4. Test Vehicle Flight Path with Base Station Node Markings

The following test parameters served as the basis for the chosen node locations:

- **Maximize Distance Between Nodes** – This tests the MESH network's extended range capability whilst simultaneously maintaining line of sight from the flight test vehicle.
- **Clear Field of View for Ground Nodes** – This minimizes multipath interference and ensures a continuous line of sight with the test plane.
- **Separation Distances** – Refer to Table 4.1 below for the approximate separation in meters between the ground nodes.
- **Communication Via Ethernet** (between the INS and BluSDR)
- **Test Conditions** – Set the following BluSDR radio parameters:
  - **Bandwidth** = 10 MHz
  - **Operating Frequency** = 2265 MHz
  - **Power Output** = 1 W

Table 4.1. Ground Node Separation

Nodes	1	3	4
1	-	6408.5 m	7052.1 m
3	6408.5 m	-	739.0 m
4	7052.1 m	739.0 m	-

5. Standard Flight Test Outcomes

The results from the conducted flight tests described in Section 4 consist of quantitative outcomes and plotted results.

5.1. RF Range Accuracy

Figure 5.1 below shows a comparison between the node separation values estimated by the RF ranges from the MESH network and the ground truth reference from multi-GNSS constellation-based position updates.

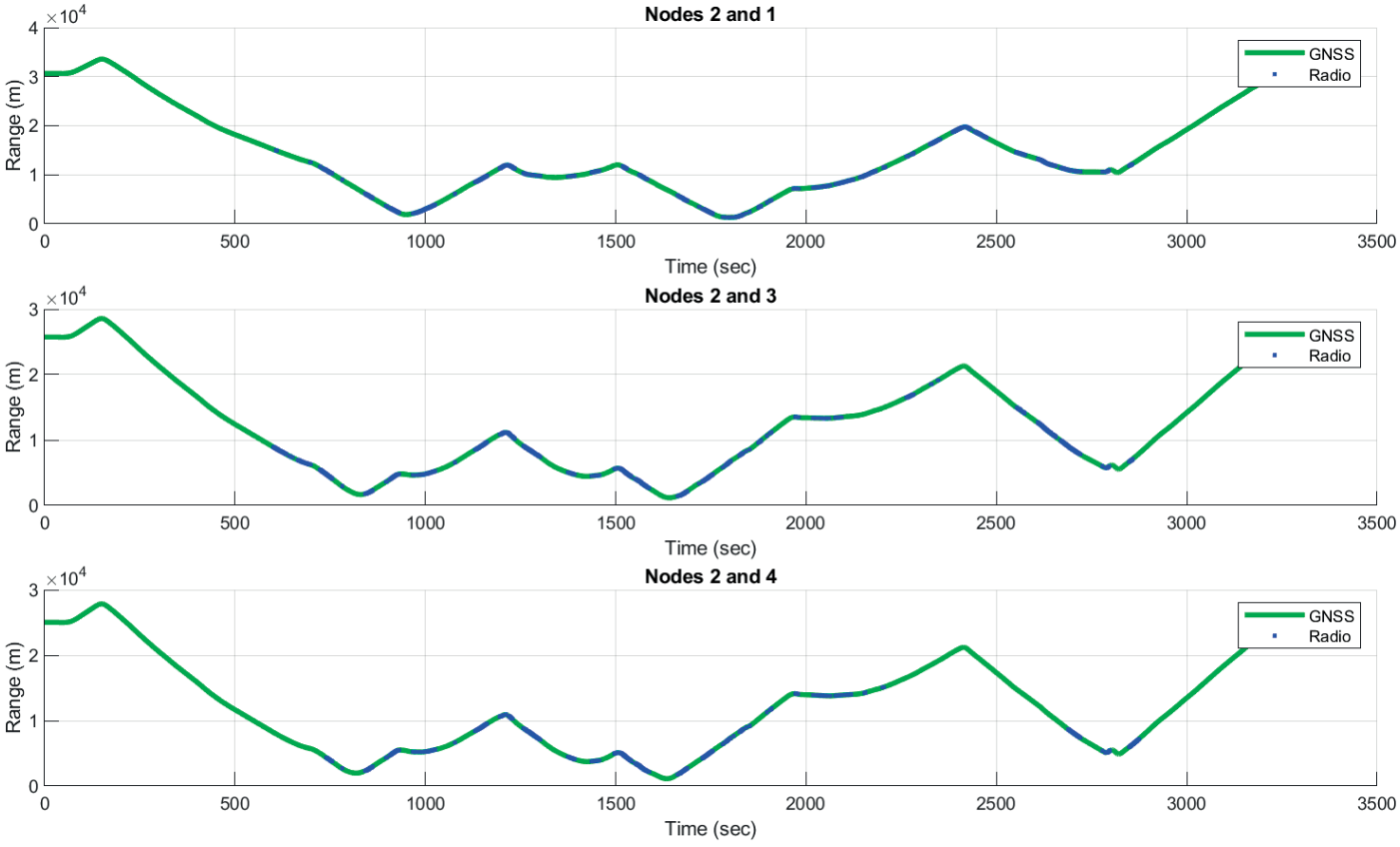


Figure 5.1. Node Range Comparison Between GNSS Reference and Real-time RF Range Estimates

5.1.1. RF Range Analysis

Radio node two represents the dynamic BluSDR-30 onboard the test airplane. Radio nodes one, three, and four are the static ground base nodes shown in Figure 4.2. The green “GNSS” plot refers to the GNSS ground truth ranges, while the blue “Radio” points refer to the RF range estimates. Note, these RF values were extracted only from the RF signals without any GNSS aiding.

Refer to Table 5.1 for the mean error results between the RF range estimates and the GNSS range computations. Note, this table concerns the node separation distance between the ground base stations displayed and radio node two onboard the test plane. The close to zero mean error values mean the RF range estimates were accurate.

Table 5.1. RF Accuracy Results

Nodes	Base 1	Base 3	Base 4
Mean Error, m	-0.5	3.2	-0.5

5.2. GNSS-Denied Position Accuracy

The tightly coupled INS solution can triangulate an accurate position estimate, which provides resilience against GNSS signal loss. This is possible when at least 2 RF ranges estimates from all ground nodes are available, and their static positions are known. Refer to Figure 5.2 below for the GNSS-denied position estimation performance of the INS when using only raw ranging updates in the tightly coupled fusion filter.

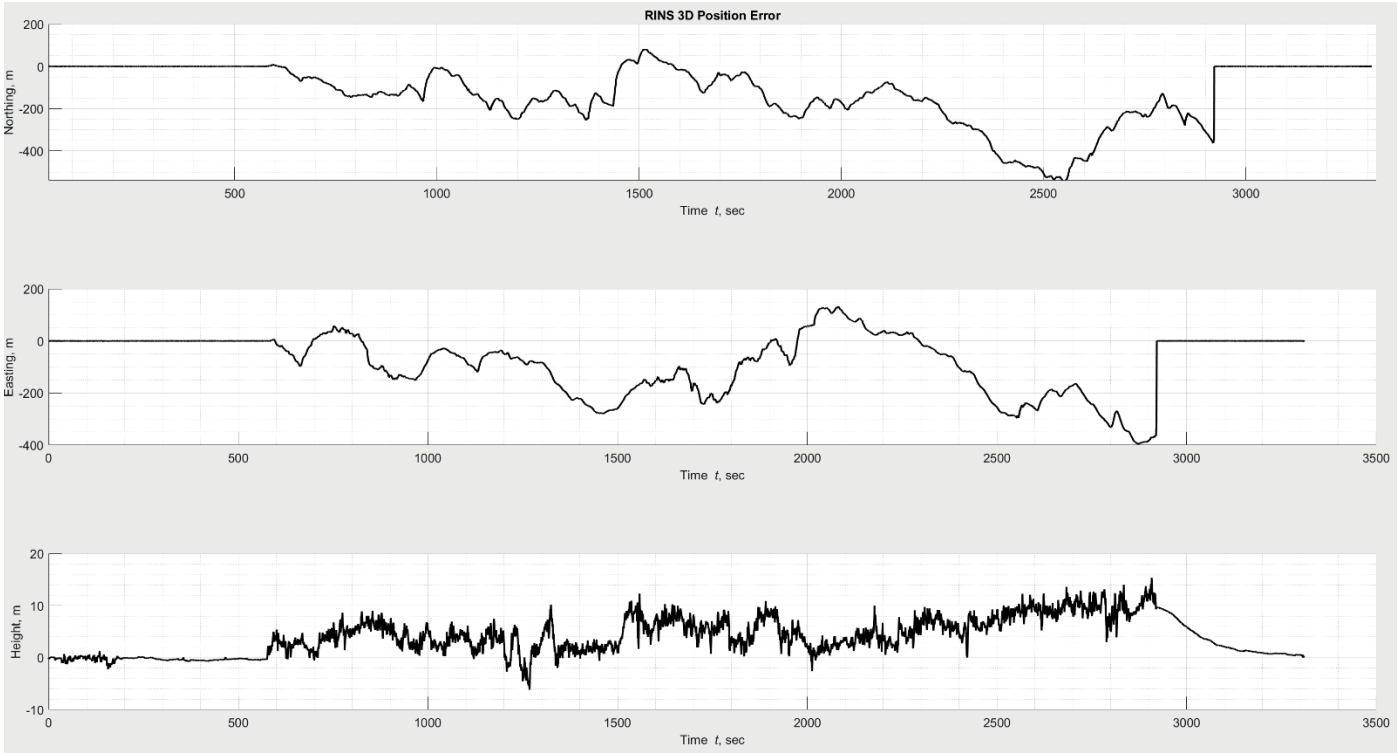


Figure 5.2. INS Position Accuracy Using RF Range Estimates

5.2.1. Position Accuracy Analysis

In the GNSS-denied scenario the RMS position error was 92 meters over the time of the flight. This demonstrates the system's ability to maintain reasonable positioning accuracy even without GNSS data. The spikes in the plot indicate instances when the radios failed to create a MESH network. As a result, the INS provided a free inertial solution on its own, causing larger position errors reflected as visible jumps in the upper two latitude and longitude error plots.

The top panel in Figure 5.2 shows the difference between the GNSS and RINS latitude values. During the GNSS-denied portion the RINS effectively handled position estimation, maintaining a steady performance without significant jumps or drifts. There were some spikes during the MESH network loss, but overall, the latitude error remained consistent.

The middle panel shows the longitude difference between the GNSS and RINS. Like the latitude error results, there were variations during the GNSS-denied periods, but the overall tracking remained aligned. The significant spikes in error coincides with the loss of the RF network, during which the INS solely provides the solution. Even with these spikes however, the system maintained its overall consistency like with latitude.

The bottom panel shows the altitude error between the GNSS and RINS. The tightly coupled filter demonstrated excellent altitude tracking even during GNSS-denied conditions. The relatively small variation in error shows the INS can maintain accurate altitude estimates. Note, the RINS altitude estimates closely followed both the GNSS and barometric altitude readings throughout the flight. Refer to Figure 5.2 for the overall error found. Refer to figure 5.3 below to see how the INS position estimates differ when GNSS is on and off.

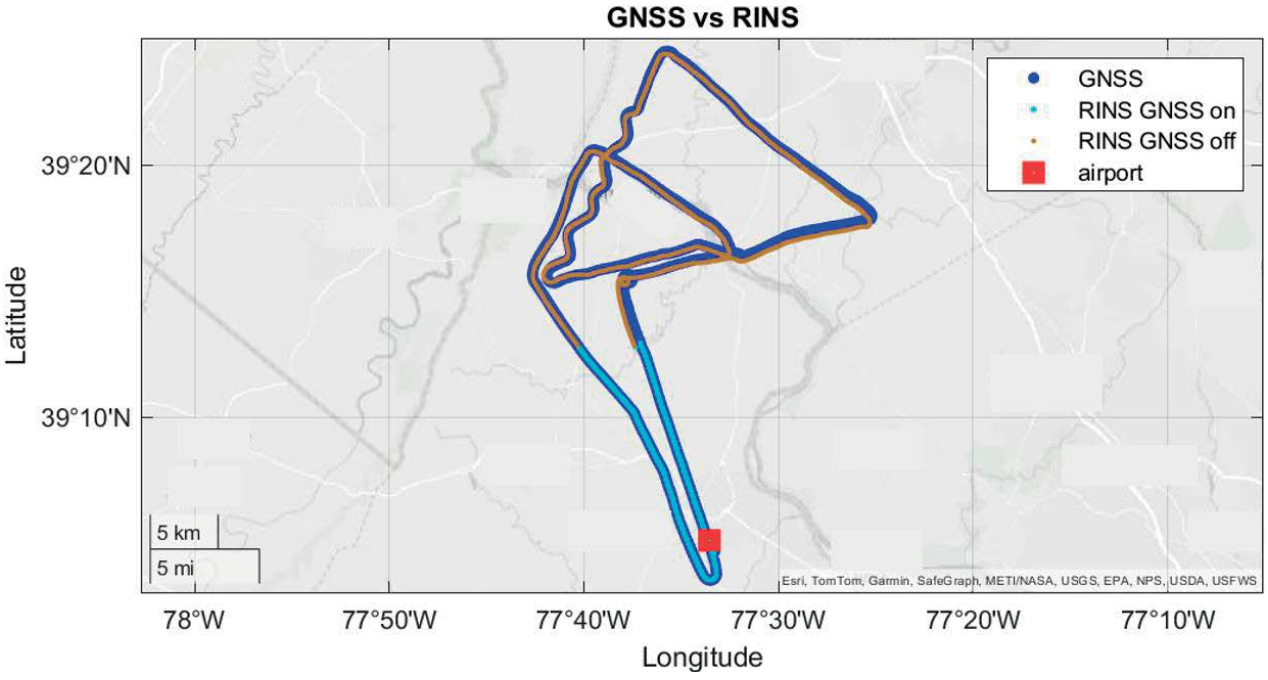


Figure 5.3. INS Position Estimates in GNSS-Enabled and Disabled Areas

In the figure shown, the reference GNSS flight path is in blue, while the INS position estimates with time-of-flight aiding data for GNSS-enabled conditions are in cyan and the GNSS-denied condition results are in brown. Note, the airport indicated by the red square represents both the start and end location of the flight path.

The error in the INS position estimates remains consistent throughout the flight with the largest deviation observable during the circular flight path pattern. Despite the deviation when GNSS is unavailable, the integration of RF ranging data with the INS limits the overall drift. This ensures the position estimates do not completely diverge from the true flight path, especially in longer GNSS-denied phases. Note, the re-enabling of GNSS aiding data allows the INS position estimates to return to the true position with error even dropping to pre-GNSS denied portions of the flight.

5.3. Range error and Range Comparison

For an overall comparison, Figure 5.4 shows the range estimation error using the RF ranging method and the separation distance between flight node two and ground nodes one, three, and four.

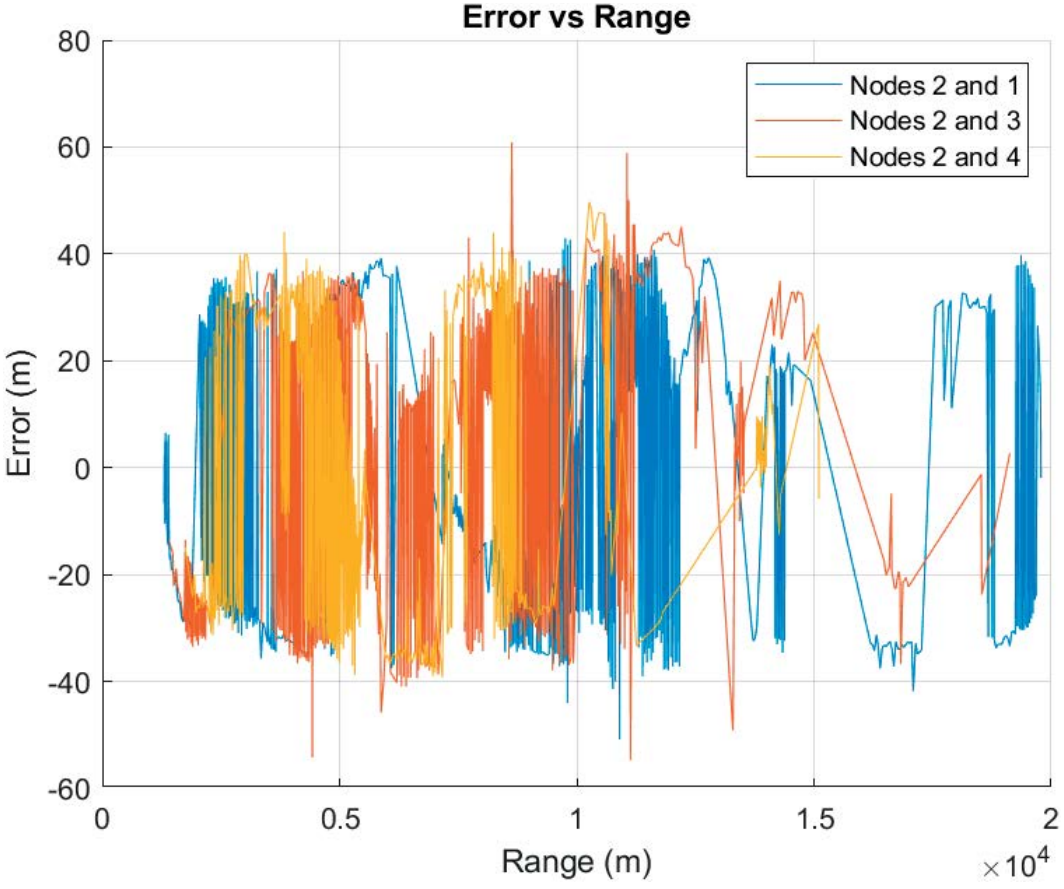


Figure 5.4. INS Position Estimation Error Using RF Ranging and Node Ranges

5.3.1. Error Analysis

From the graph, it is apparent that the error does not strongly correlate with the increasing range between the nodes and is instead more dependent on the environmental or signal conditions. Node pairs two and three shown in orange, as well as node pairs two and four shown in yellow, exhibit more frequent and larger deviations in error compared to node pair two and one shown in blue. The blue pair shows more stable error values overall, and especially at longer ranges. This may suggest that nodes two and one have a stronger or clearer signal path, which leads to more accurate range estimates.

Certain portions of the data show negative errors. This indicates instances when the system underestimated the range. These sections could be the result of environmental factors, such as signal multipath interference or occlusions affecting the radio signal between nodes. Additionally, the graph shows spikes in errors up to 60 meters high. This suggests moments when the signal quality was particularly degraded. This could be due to interference or obstacles between the nodes. However, even at higher ranges the error seems to stabilize, especially for the blue node pairs.

6. Flight Test Results Using Two Radios

This test sought to evaluate the performance of the system using only two radios set seven kilometers apart, rather than the standard three or more stations. Despite the reduction in radio nodes, the system maintained suitable position estimation accuracy. These results show promising results in GNSS-denied environments.

6.1. Radio Node Placement

The radios were strategically positioned to maximize the distance between the radio nodes, while still maintaining a clear line of sight to the test aircraft. This setup provided strong results despite involving fewer nodes than typically.

Figure 6.1 below shows the chosen locations for both radios, as well as the flight path for the test plane.

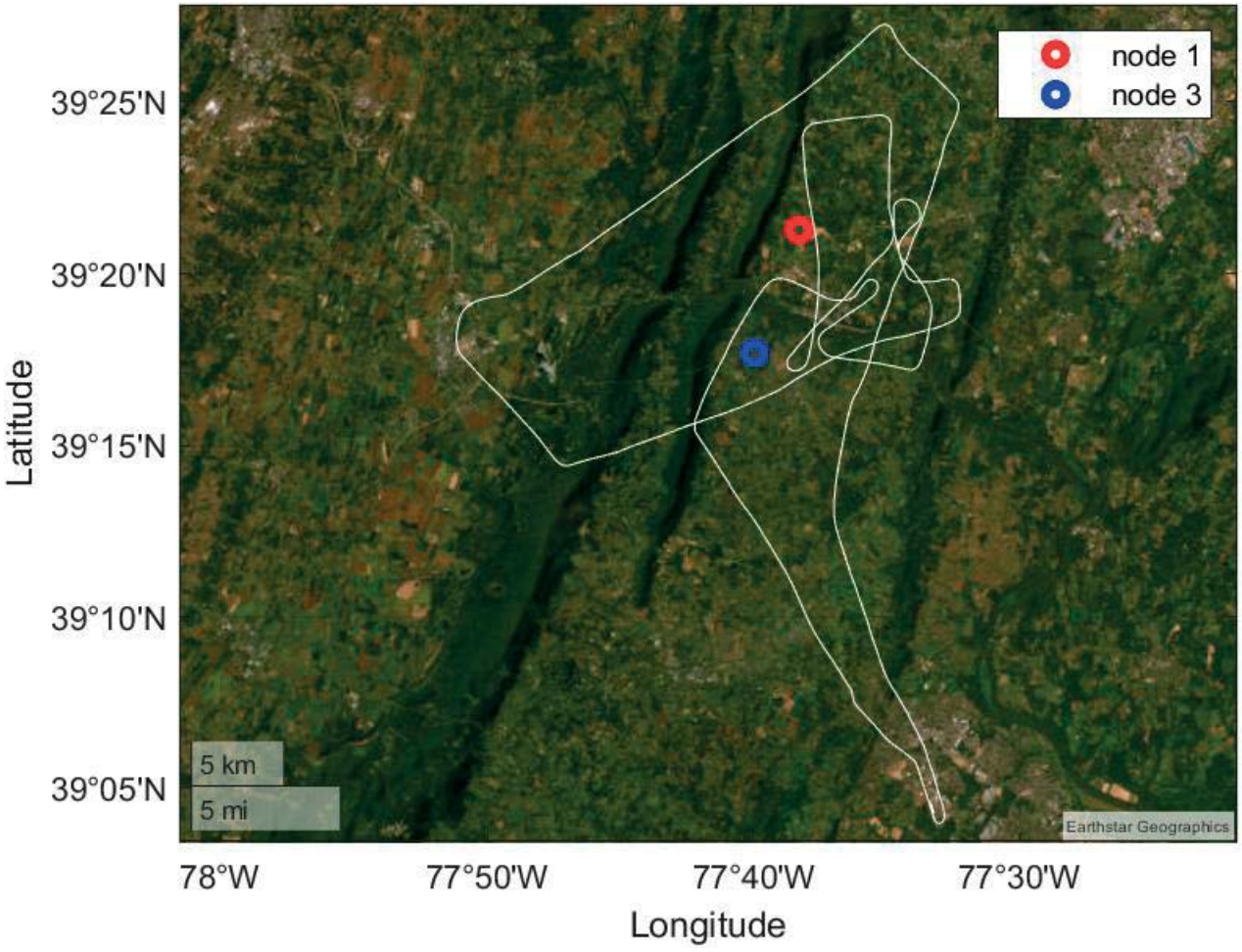


Figure 6.1. Radio Node Locations

Refer to Figure 6.2 below to see how the INS position estimates differ when GNSS is on and off.

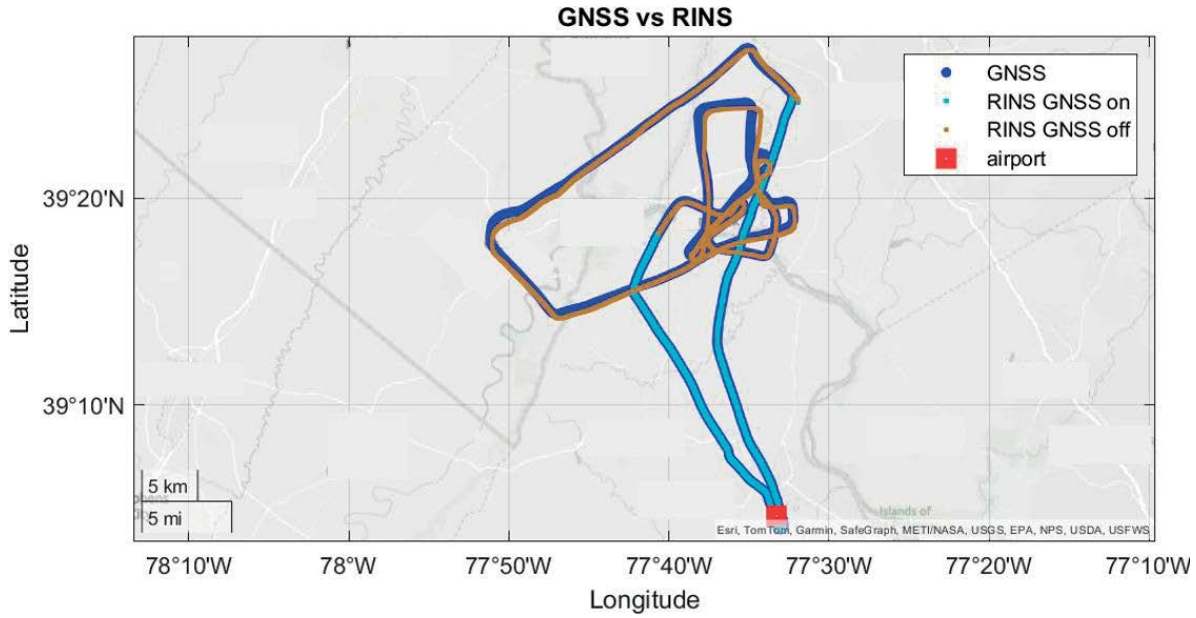


Figure 6.2. INS Position Estimates in GNSS-Enabled and Disabled Areas

6.1.1. Range Error Analysis

The following plots illustrate the comparison between radio-based range estimates with GNSS-derived ground truth. Figure 6.3 shows the time-based error analysis comparing the range error between the blue node pair (2 and 1) and the red node pair (2 and 3).

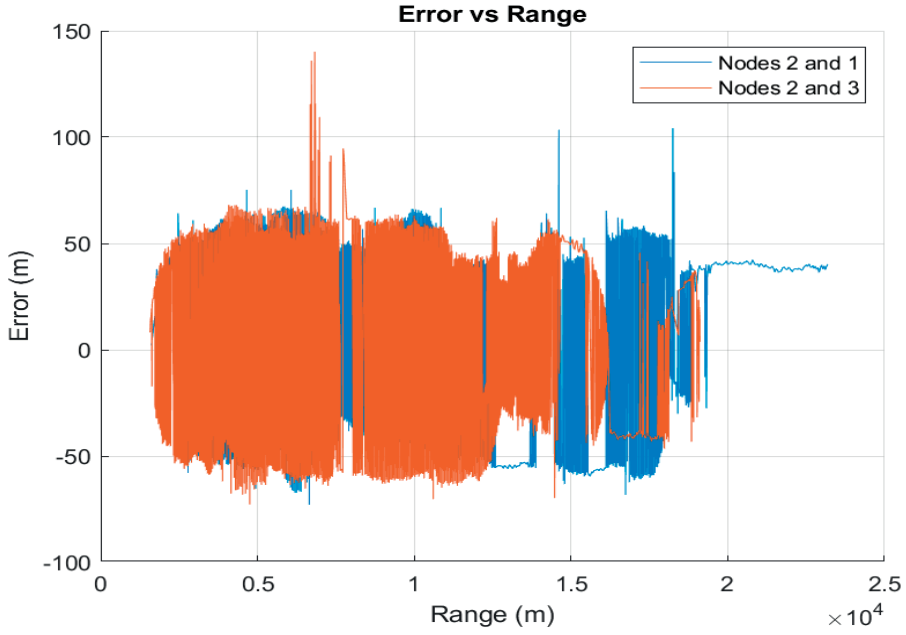


Figure 6.3. INS Position Estimation Error Using RF Ranging and 2 Node Ranges

The plot shows that the error tends to stabilize as the distance between the radios increases. This confirms the system maintains acceptable accuracy even with fewer nodes.

Despite using only two radios, the range estimates were close to the GNSS ground truth. This highlights the system's ability to function accurately even in scenarios with a reduced number of radios. Figure 6.4 below shows a direct comparison between the green GNSS estimates and the blue radio range estimates for node pairs 2 & 1, as well as node pairs 2 & 3.

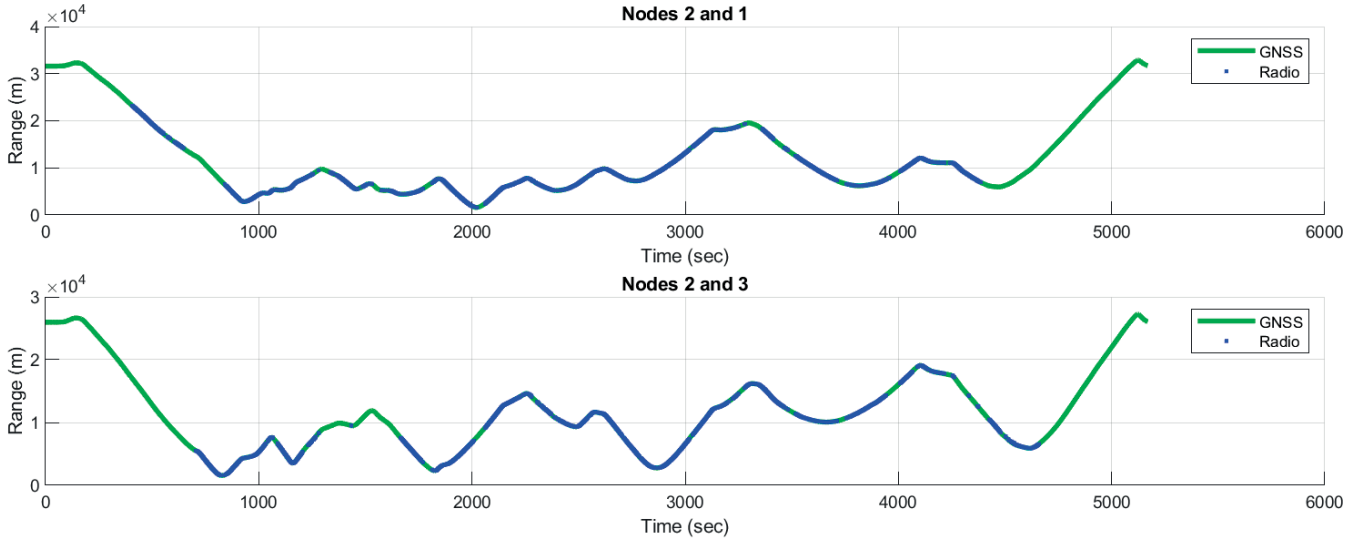


Figure 6.4. Comparison Between GNSS and Radio Range Estimates

6.2. INS Position Error

Despite only using two radios during this test, the error results shown in Figure 6.5 remain within the 200-meter bound, moreover the RMS error over time was 100 meters for the 3D position. The occasional peaks shown to exceed this bound correspond to moments when the mesh network was not yet fully formed. However, the system quickly recovered and maintained a tightly bounded accuracy throughout the duration of the test.

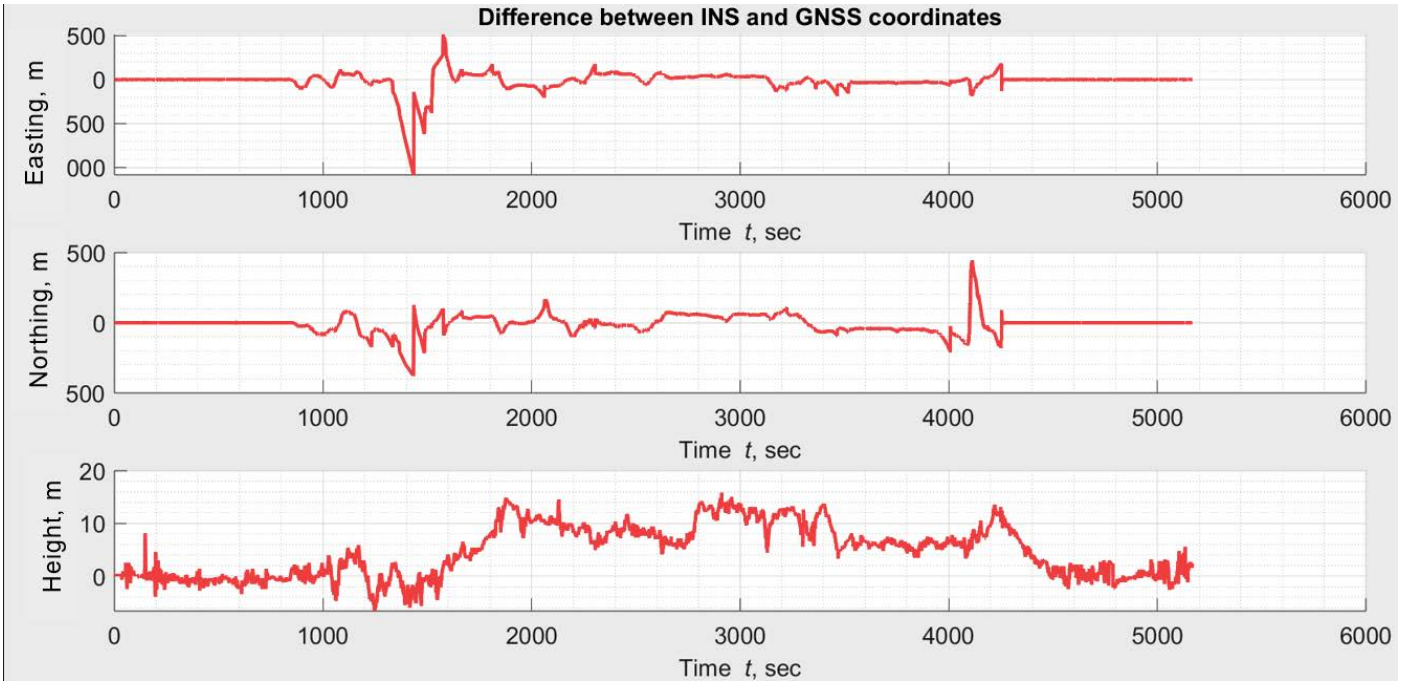


Figure 6.5. INS Position Error Using Two Radios

Overall, in this second test, the system achieved a continuous and solid mesh between the two radios. Despite adverse weather conditions, the network remained stable and further enhanced the system's accuracy. The system's position estimates shown in Figure 6.5 remained accurate. The mean error in GNSS-denied conditions was ~200 meters over time even in the challenging environmental experiences.

7. Conclusion

The results of the RINS system in GNSS-denied environments demonstrate the system's superior performance and reliability. Integrating visual data and inertial measurements allows the RINS to create a resilient solution to bridge the gap in situations where GNSS signals are unavailable. This ability to seamlessly provide precise altitude, latitude, and longitude data during GNSS outages is a critical advantage for both safety and operational success in aviation and other fields.

In summary, the RINS performance in GNSS-denied environments highlights its strength as a dependable alternative navigation solution. Whether for unmanned aerial vehicles, autonomous systems, or other applications where GNSS signals may be disrupted, the RINS maintains accurate navigation. Its effectiveness in mitigating drift and its resilient design ensures that it is an exemplary solution for GNSS-denied scenarios.

8. Bibliography

1. T. Morong, Pavel Puričer, and Pavel Kovář, “Study of the GNSS Jamming in Real Environment,” International Journal of Electronics and Telecommunications, Jul. 2023, doi: https://doi.org/10.24425/ijet.2019.126284.

2. A. J. Kerns, D. P. Shepard, J. A. Bhatti, and T. E. Humphreys, “Unmanned Aircraft Capture and Control Via GPS Spoofing,” Journal of Field Robotics, vol. 31, no. 4, pp. 617–636, Apr. 2014, doi: https://doi.org/10.1002/rob.21513.

8. Revision History

Table 8.1. Change Status Log

Revision	Date	Affected paragraphs	Remarks
1.0	Sep.11, 2024	All	Initial release
1.2	Sep. 18, 2024	All	Adjusted plots for readability and added additional plot.
1.3	Sep. 23, 2024	All	Refined definition of error for clarity and replaced graphics for higher quality versions.
1.4	Sep. 27, 2024	All	Released version.
1.5	Oct. 03, 2024	4.2, 5.1,5.2	Adjustments and parameters correction
1.6	Nov. 13, 2024	All	Wording and figure adjustments

Contact Us: +1 (703) 880-4222 | (+1 844 468 4284).

Address: 39959 Catoctin Ridge Street, Paeonian Springs, VA 20129 U.S.A.